Inorganic Chemistry

Dimanganese and Diiron Complexes of a Binucleating Cyclam Ligand: Four-Electron, Reversible Oxidation Chemistry at High Potentials

Louise A. Berben and Jonas C. Peters*

Department of Chemistry, Massachusetts Institute of Technology, Cambridge, Massachusetts 02139

The reaction of a binucleating biscyclam ligand cyclam$_2^i$PrO [where cyclam$_2^i$PrO = (1,3-bis[1,4,8,11-tetraazacyclododecane]-2-hydroxypropane] with Mn(CF$_3$SO$_3$)$_2$ or Fe(CF$_3$SO$_3$)$_2$·2MeCN gives [(cyclam$_2^i$PrO)Mn$_2$(μ-CF$_3$SO$_3$)](CF$_3$SO$_3$)$_2$ (**4**) and [(cyclam$_2^i$PrO)Fe$_2$(μ-CF$_3$SO$_3$)](CF$_3$SO$_3$)$_2$ (**6**), respectively. [(cyclam$_2^i$PrO)Mn$_2$(μ-N$_3$)](CF$_3$SO$_3$)$_2$ (**5**) is obtained by the reaction of **4** with NaN$_3$. Single-crystal X-ray structural characterization indicates that in each of the bimetallic complexes the two metal centers are facially coordinated by a cyclam ligand and bridged by the isopropoxide linker of the ligand in addition to a triflate counteranion. Upon replacement of the triflate bridge with the single-atom bridge of an end-bound azide ligand in **5**, the Mn—Mn distance decreases by 0.38 Å. All of the complexes are high-spin and colorless and were characterized by magnetic susceptibility measurements, electron paramagnetic resonance spectroscopy, and electrochemical methods. Magnetic susceptibility measurements indicate that **4** and **6** are weakly antiferromagnetically coupled while **5** is weakly ferromagnetically coupled. Cyclic voltammetry measurements indicate that the hard donor amine ligands impart high oxidation potentials to the metal centers and that four-electron redox activity can be accessed with a narrow potential range of 0.72 V. Upon inclusion of water in the cyclic voltammetry experiment, the oxidative waves shift to higher potentials, which is consistent with water binding the manganese centers. The diiron complex **6** displays four one-electron redox couples, of which the final two are irreversible. Inclusion of water in the cyclic voltammetry measurement for compound **6** resulted in two sets of shifted peaks, which suggests that two molecules of water bind the diiron core. In accordance with the observed reversibility of the electrochemical results, the dimanganese complex is more efficient than the diiron complex for mediating O-atom transfer to organic substrates and is an excellent hydrogen peroxide disproportionation catalyst, with the reaction proceeding for over 20 000 turnovers.

Introduction

Recent proposals for the mechanism of dioxygen formation by photosystem II invoke oxidation of water to form a Mn^{V}O species followed by nucleophilic attack of a calcium-bound water molecule on the Mn^{V}oxo moiety, leading to the formation of the O—O bond of dioxygen. An alternate proposal involves O—O bond formation via coupling of Mn^{IV}oxo species that have radical character with a calcium-bound hydroxide substrate.[1] In synthetic systems, architectures that target both of these scenarios have been targeted, including studies of the ruthenium "blue dimer" reported by Meyer and co-workers.[2] Of increasing interest is the study of multimetallic systems that can access four-electron redox

chemistry at high potentials in which the molecular architectures and electronic structures facilitate the formation of high-valent metal—oxo moieties poised for radical coupling.

We are involved in a collaborative effort directed at developing catalysts for the oxidation of water that, in conjunction with a solar-powered charge-separating device

(1) (a) Siegbahn, P. E. M.; Crabtree, R. H. *J. Am. Chem. Soc.* **1999**, *121*, 117. (b) Iwata, S.; Barber, J. *Curr. Opin. Struct. Biol.* **2004**, *14*, 447. (c) Ferreira, K. N.; Iverson, T. M.; Maghlaoui, K.; Barber, J.; Iwata, S. *Science* **2004**, *33*, 1831. (d) Yano, J.; Kern, J.; Sauer, K.; Latimer, M. J.; Pushkar, J.; Biesiadka, J.; Loll, B.; Saenger, W.; Messinger, J.; Zouni, A.; Yachandra, V. K. *Science* **2006**, *314*, 821. (e) Siegbahn, P. E. M. *Chem.—Eur. J.* **2006**, *12*, 9217. (f) Sauer, K.; Yano, J.; Yachandra, V. K. *Coord. Chem. Rev.* **2008**, *252*, 318. (g) Dasgupta, J.; Ananyev, G. M.; Dismukes, G. C. *Coord. Chem. Rev.* **2008**, *252*, 347. (h) Yano, J.; Yachandra, V. K. *Inorg. Chem.* **2008**, *47*, 1711.
(2) (a) Binstead, R. A.; Chronister, C. W.; Ni, J.; Hartshorn, C. M.; Meyer, T. J. *J. Am. Chem. Soc.* **2000**, *122*, 8464. (b) Hurst, J. K. *Chem. Rev.* **2005**, *249*, 313. (c) Cady, C. W.; Crabtree, R. H.; Brudvig, G. W. *Coord. Chem. Rev.* **2008**, *252*, 444.

* To whom correspondence should be addressed. E-mail: jcpeters@mit.edu

and a proton reduction catalyst, might be able to store solar energy in the form of chemical bonds.[3] In this context, bimetallic complexes of iron and manganese are of interest in order to study their multielectron redox properties at high potentials and possible bimetallic oxo structures and associated reactivity. Evidence for the radical nature of high-valent nonheme iron−oxo complexes has been obtained from detailed structural and spectrosopic studies of less reactive inorganic complexes.[4−6] In particular, studies on [(TMC)Fe^{IV} =O]$^{2+}$ (TMC = 1,4,8,11-tetramethyl-1,4,8,11-tetraazacyclododecane) have yielded interesting reactivity and structural information.[5] Spectroscopic and density functional theory (DFT) studies have shown that in [(TMC)Fe^{IV}=O(MeCN)]$^{2+}$ the highly covalent Fe−O π bond is the origin of significant unpaired electron spin density (0.77e$^-$) on the O atom.[6]

In contrast, studies of similar nonheme manganese systems have yielded a class of highly active epoxidation and *cis*-dihydroxylation catalysts.[7] Structurally characterized manganese−oxo species have only been obtained in the presence of stabilizing, anionic ligands presumably due to the higher oxidation power of high-valent manganese as compared to iron.[8,9] While many dimeric manganese complexes have been synthesized in which the manganese centers are bridged by oxo, hydroxo, or alkoxo ligands, very few display four-electron, reversible electrochemistry; we are aware of only one example of a dimanganese complex, [(Mn(bpia)(Cl))$_2$(μ-O)](ClO$_4$)$_2$·2MeCN [where bpia = bis(picolyl)(*N*-methylimidazol-2-yl)amine], in which oxidation states spanning four-electron redox activity (ranging from Mn$^{II}_2$ to Mn$^{IV}_2$) could be reversibly accessed.[10,11] A larger number of dimanganese complexes are capable of three-electron, re-

versible redox chemistry,[12] and many display fewer or irreversible redox events. In addition to achieving four-electron, reversible oxidation chemistry at potentials high enough to oxidize water (0.815 V at pH = 7, NHE), another challenging problem in multielectron redox reactivity is constraining the spread of the successive oxidation potentials to a narrow range; in [(Mn(bpia)(Cl))$_2$(μ-O)](ClO$_4$)$_2$·2MeCN, these redox couples are spread over 0.91 V.[10]

In this work, we report the synthesis of a binucleating cyclam (cyclam = 1,4,8,11-tetraazacyclododecane) ligand and examples of its diiron and dimanganese coordination complexes. Cyclic voltammetry measurements indicate that four-electron redox activity at high potentials can be accessed. We show that for the dimanganese complex the redox events are all reversible, with the most positive two-electron couple occurring at 1.5 V vs SCE. In accordance with the comparative redox chemistry of the iron and manganese complexes, we observed that the dimanganese complex is more efficient than the diiron complex at mediating O-atom transfer to organic substrates. The dimanganese complex also displays highly efficient catalase activity.

Results and Discussion

Synthesis of Ligands and Complexes 1−6. The binucleating cyclam ligand 1,3-bis(cyclam)-2-hydroxypropane, henceforth denoted cyclam$_2^i$PrOH or **3**, was accessed via a synthetic route similar to that used in the synthesis of other linked bisazamacrocycle ligands including the related amine-donor ligand 1,3-bis(tacn)-2-hydroxypropane (tacn = 1,4,7-triazacyclononane) originally synthesized by Sessler and co-workers.[13] In this case, the Boc-protected (where Boc = *tert*-butyloxycarbonyl) presursor to cyclam$_2^i$PrOH, 1,3-bis(Boc$_3$-cyclam)-2-hydroxypropane (**1**), was obtained in 45% yield by the reaction of triply Boc-protected cyclam with 1,3-dibromo-2-hydroxypropane in the presence of triethylamine followed by purification by column chromatography (Scheme 1). Acid-mediated deprotection of **1** to yield the nonahydrochloride salt of the ligand (**2**) followed by neutralization of an aqueous solution of **2** provided the free ligand **3** as a white powder.

The reaction of a suspension of **3** in acetonitrile with 2 equiv of Mn(CF$_3$SO$_3$)$_2$ and 1 equiv of Et$_3$N dissolved in acetonitrile at room temperature afforded [(cyclam$_2^i$PrO)Mn$_2$(μ-

(3) Powering the Planet: A Chemical Bonding Center. Website: http://www.caltechmitsolarpower.caltech.edu.

(4) (a) Lim, M. H.; Rohde, J.-U.; Stubna, A.; Bukowski, M. R.; Costas, M.; Ho, R. Y. N.; Münck, E.; Nam, W.; Que, L., Jr. *Proc. Natl. Acad. Sci. U.S.A.* **2003**, *100*, 3665. (b) Tiago de Oliveira, F.; Chanda, A.; Banerjee, D.; Shan, X.; Mondal, S.; Que, L., Jr.; Bominaar, E. L.; Münck, E.; Collins, T. J. *Science* **2007**, *315*, 835. (c) Pestovsky, O.; Stoian, S.; Bominaar, E. L.; Shan, X.; Münck, E.; Que, L., Jr.; Bakac, A. *Angew. Chem., Int. Ed.* **2005**, *44*, 6871. (d) Kaizer, J.; Klinker, E. J.; Oh, N. Y.; Rohde, J.-U.; Song, W. J.; Stubna, A.; Kim, J.; Münck, E.; Nam, W.; Que, L., Jr. *J. Am. Chem. Soc.* **2004**, *126*, 472. (e) Berry, J. F.; Bill, E.; Bothe, E.; Neese, F.; Weighardt, K. *J. Am. Chem. Soc.* **2006**, *128*, 13515.

(5) Rhode, J.-U.; In, J.-H.; Lim, M. H.; Brennessel, W. W.; Bukowski, M. R.; Stubna, A.; Münck, E.; Nam, W.; Que, L., Jr. *Science* **2003**, *299*, 1037.

(6) Decker, A.; Rhode, J.-U.; Que, L., Jr.; Solomon, E. I. *J. Am. Chem. Soc.* **2004**, *126*, 5378.

(7) (a) Jacobsen, E. N.; Wu, M. H. Epoxidation of Alkenes Other Than Allylic Alcohols. In *Comprehensive Asymmetric Catalysis*; Jacobsen, E. N., Pfaltz, A., Yamamoto, H., Eds.; Springer: New York, 1999; pp 649−677. (b) Groves, J. T. *J. Inorg. Biochem.* **2006**, *100*, 434. (c) Nam, W. *Acc. Chem. Res.* **2007**, *40*, 522.

(8) (a) Collins, T. J.; Gordon-Wylie, S. W. *J. Am. Chem. Soc.* **1989**, *111*, 4511. (b) MacDonnell, F. M.; Fackler, N. L. P.; Stern, C.; O'Halloran, T. V. *J. Am. Chem. Soc.* **1994**, *116*, 7431.

(9) (a) Manganese−oxo species stabilized by hydrogen-bonding interactions have been characterized. For example, see: Parsell, T. H.; Behan, R. K.; Green, M. T.; Hendrich, M. P. Borovik, A. S. *J. Am. Chem. Soc.* **2006**, *128*, 8728. (b) MacBeth, C. E.; Gupta, R.; Mitchell-Koch, K. R.; Young, V. G.; Lushington, G. H.; Thompson, W. H.; Hendrich, M. P.; Borovik, A. S. *J. Am. Chem. Soc.* **2004**, *126*, 2556.

(10) Triller, M. U.; Hseih, W.-Y.; Pecoraro, V. L.; Rompel, A.; Krebs, B. *Inorg. Chem.* **2002**, *41*, 5544.

(11) Four-electron, reversible redox chemistry has also been observed in trinuclear manganese complexes. For example, see: Birkelback, F.; Floerke, U.; Haupt, H.-J.; Butzlaff, C.; Trautwein, A. X.; Wieghardt, K.; Chaudhuri, P. *Inorg. Chem.* **1998**, *37*, 2000.

(12) (a) For example, see: Pessiki, P. J.; Khangulov, S. V.; Ho, D. M.; Dismukes, G. C. *J. Am. Chem. Soc.* **1994**, *116*, 891. (b) Gelasco, A.; Kirk, M. L.; Kampf, J. W.; Pecoraro, V. L. *Inorg. Chem.* **1997**, *36*, 1829. (c) Gelasco, A.; Pecoraro, V. L. *Inorg. Chem.* **1998**, *37*, 3301. (d) Lomoth, R.; Huang, P.; Zheng, J.; Sun, L.; Hammarstroem, L.; Akermark, B.; Styring, S. *Eur. J. Inorg. Chem.* **2002**, 2965. (e) Baffert, C.; Collomb, M.-N.; Deronzier, A.; Kjaergaard-Knudson, S.; Latour, J.-M.; Lund, K. H.; McKenzie, C. J.; Mortensen, M.; Nielsen, L. P.; Thorup, N. *Dalton Trans.* **2003**, 1765. (f) Magnuson, A.; Liebisch, P.; Hoegblom, J.; Anderlund, M. F.; Lomoth, R.; Meyer-Klaucke, W.; Haumann, M.; Dau, H. *J. Inorg. Biochem.* **2006**, *100*, 1234. (g) Pecoraro, V. L.; Hsieh, W.-Y. *Inorg. Chem.* **2008**, *47*, 1765.

(13) (a) Sessler, J. L.; Sibert, J. W.; Burrell, A. K.; Lynch, V.; Markert, J. T.; Wooten, C. L. *Inorg. Chem.* **1993**, *32*, 4277. (b) Iranzo, O.; Elmer, T.; Richard, J. P.; Morrow, J. R. *Inorg. Chem.* **2003**, *42*, 7737.

Scheme 1. Synthesis of **3**
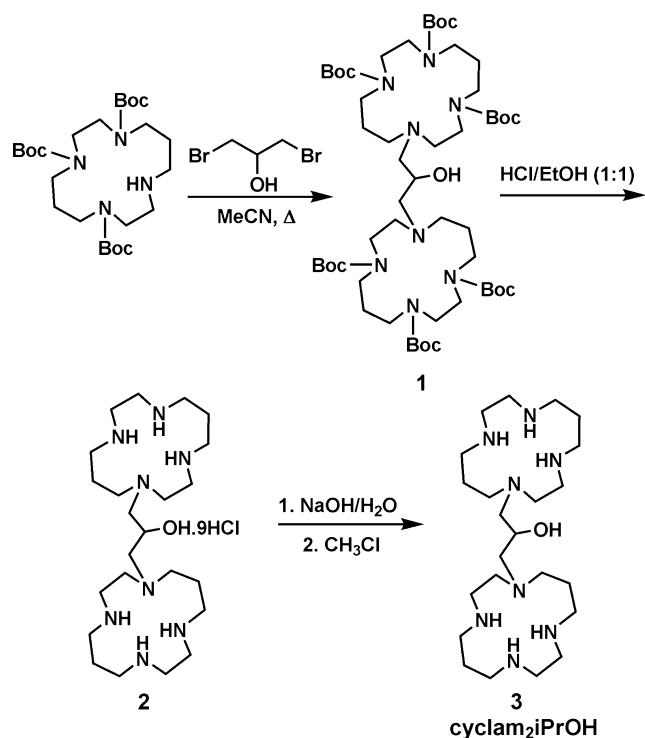
CF$_3$SO$_3$)](CF$_3$SO$_3$)$_2$ (**4**), which could be isolated as colorless block-shaped crystals by diffusion of ether vapor into acetonitrile (Scheme 2). The exclusion of air and moisture in all complex syntheses proved necessary to avoid the formation of oily, intractable products. Anion-exchange reactions with complex **4** proved facile. Reaction with NaN$_3$ yielded [(cyclam$_2$^{i}PrO)Mn$_2$(μ-N$_3$)](CF$_3$SO$_3$)$_2$ (**5**). The structures of both dimanganese complexes were confirmed by X-ray structure determinations as described below (Figures 1 and 2). IR spectroscopic evidence was also obtained for the formation of CN$^-$ and NO$_2$$^-$ adducts anaolgous to compound **5** via the reaction of **4** with NaCN and NaNO$_2$, respectively.

The analogous diiron complex [(cyclam$_2$^{i}PrO)Fe$_2$(CF$_3$SO$_3$)](μ-CF$_3$SO$_3$)$_2$ (**6**) was obtained by the addition of **3** dissolved in methanol to 2 equiv of Fe(CF$_3$SO$_3$)$_2$·2MeCN in methanol, followed by crystallization by diffusion of ether into the filtered reaction mixture. Because of the high-spin d^5 and d^6 electronic configurations of the manganese(II) and iron(II) complexes, neither NMR nor UV−visible spectroscopy was informative for characterization purposes; elemental analysis data, variable-temperature magnetic susceptibility measurements, and electron paramagnetic resonance (EPR) spectrocopy confirmed the electronic structure and purity of the complexes, which were identified and characterized by single-crystal X-ray crystallography (vide infra).

Solid-State Structures of 4−6. Single crystals of all three complexes were obtained by diffusion of ether into MeCN or MeOH solution. The solid-state structures of **4** and **6** are isostructural (Figure 1). Both structures reveal two M(II) centers (where M = Mn or Fe), each ligated by one tetradentate cyclam ligand and bridged by the O$^-$ anion of the isopropoxide linker of cyclam$_2$^{i}PrO$^-$. The sixth coordina-

tion site on each pseudo-octahedral manganese or iron center is occupied by a triflate counteranion that bridges the two metal centers. Metal−ligand bond distances in the diiron complex are slightly shorter than the corresponding distances in the dimanganese complex, in accordance with the smaller ionic radius of Fe^{II} (0.78 Å) vs Mn^{II} (0.83 Å).[14] In both **4** and **6**, the M−N distances to the cyclam ligands are all roughly equivalent. In each case, the M−N(4) bond trans to the M−O(1) bond is slightly longer than the other M−N distances as a result of a weak trans influence. The Mn---Mn and Fe---Fe separations in the complexes are quite long at 3.844(3) and 3.778(7) Å, respectively; combined with the M−O−M angles of 128.6(4)° and 136.7(5)° for **4** and **6**, respectively, the data indicate a wide, open binding pocket. In addition, the bridging triflate counteranion is bound on one side of the plane defined by the M−O(1)−M unit such that one face of the binding pocket remains open.

It has previously been demonstrated that in the design of binucleating ligand systems it is important that the ligand is flexible in order to accommodate metal−ligand bond length changes to accommodate changes in metal oxidation states as well as changes in the metal−metal distance upon binding of various substrates; a rigid ligand environment can prevent access to multiple oxidation states for a bound metal center.[15] The solid-state structure of **5** (Figure 2) confirms that cyclam$_2$^{i}PrO$^-$ is a very flexible ligand. The Mn---Mn distance in these complexes decreases by 0.38 Å compared with compound **4** in order to accommodate the one-atom bridge of the N$_3$$^-$ ligand [Mn---Mn is 3.461(3) Å]. The corresponding Mn−O(1)−Mn angle and Mn−O(1) distance are very similar at 129.1(5)° and 2.03(1) Å, while the Mn−N distances to the cyclam ligand have decreased slightly from an average of 2.292(3) Å in **4** to 2.211(8) Å in **5** as the metal center contracts slightly into the plane of the cyclam ring. In contrast to the binding motif of the triflate bridging anion in compounds **4** and **6**, the azide ligand lies in the same plane as the Mn−O(1)−Mn moiety.

Electronic Structure. Magnetic susceptibility measurements performed on compounds **4**−**6** revealed the presence of weak magnetic coupling between two high-spin metal ions (Table 3). For the dimanganese compounds **4** and **5** (Figure 3), the room temperature $\chi_M T$ values of 8.0 and 8.2 emu K mol^{-1}, respectively, are slightly lower than the calculated value of 8.5 emu K mol^{-1} for two isolated high-spin d^5 octahedral $S = {}^5/_2$ manganese(II) centers. For **4**, the value of $\chi_M T$ falls to 0.19 emu K mol^{-1} at 4 K, and a fit to the data using *MAGFIT3.0*[16] and a Hamiltonian of the form $\hat{H} = -2J\hat{S}_{Mn(1)}\cdot\hat{S}_{Mn(2)}$ yielded a value for the exchange coupling of $J = -3.6$ cm^{-1}. As is commonly observed for end-bound azide-bridged bimetallic complexes, compound **5** exhibited weak ferromagnetic coupling.[17] In this case, $\chi_M T$ rises at low
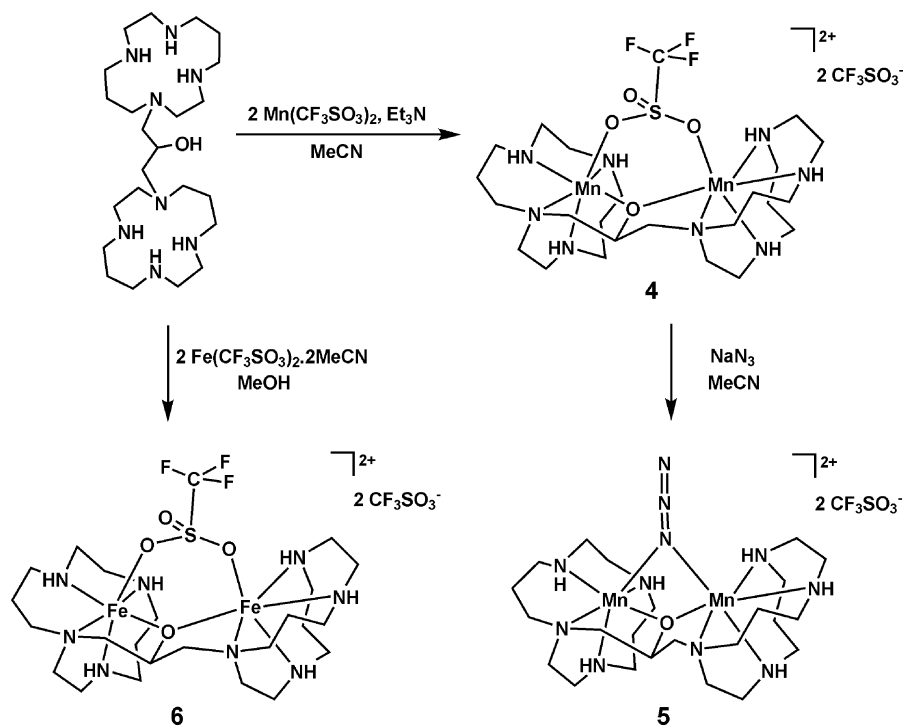
(14) (a) Bondi, A. *J. Phys. Chem.* **1964**, *68*, 441. (b) Shannon, R. D. *Acta Crystallogr., Sect. A* **1976**, *32*, 751.
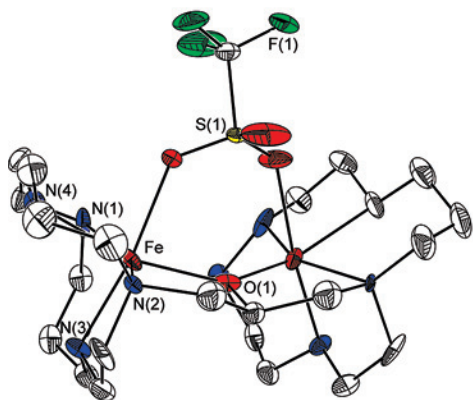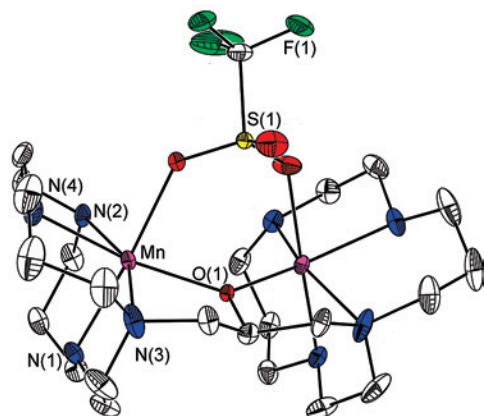(15) Bosnich, B. *Inorg. Chem.* **1999**, *38*, 2554.
(16) Schmitt, E. A. Ph.D. Thesis, University of Illinois at Urbana-Champaign, Urbana, IL, 1995.
(17) Carlin, R. L. *Magnetochemistry*; Springer-Verlag: Berlin, Germany, 1986; p 90.

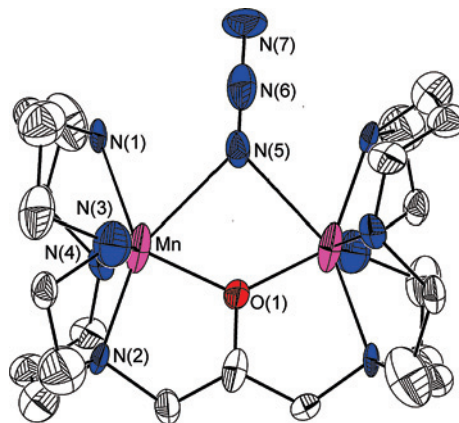**Scheme 2.** Synthesis of Dimanganese and Diiron Complexes **4**−**6**

temperature to 9.9 emu K mol^{-1}, and a fit to the data yielded a value for the exchange coupling of $J = +0.1$ cm^{-1}.

For both of the dimanganese complexes, the magnetic data were consistent with $g = 2$, as expected for the isotropic high-spin d^5 electronic configuration. Confirmation of this result for compound **4** was obtained from X-band EPR measurements. Figure 4 shows the 9.86 GHz EPR spectrum recorded at 77 K as a 1 mM methanol/toluene (1:1) solution. The 7000 G wide spectrum (Figure 4, bottom) contains a group of symmetric intense transitions centered at $g = 2$, which is characteristic of an exchange-coupled dimanganese(II) complex with weak zero-field splitting.[18] A more detailed view of the spectrum around $g = 2$ is shown in Figure 4 (top); the observed hyperfine coupling of 42 ± 3 G, approximately half of that usually observed for mononuclear manganese complexes, is also consistent with two exchange-coupled ^{55}Mn ions, which have a nuclear spin of $I = \frac{5}{2}$.

Figure 1. Structure of [(cyclam$_2$^{i}PrO)Mn$_2$(μ-CF$_3$SO$_3$)]$^{2+}$ and [(cyclam$_2$^{i}PrO)Fe$_2$(μ-CF$_3$SO$_3$)]$^{2+}$ in **4** and **6**. Purple, brown, green, red, yellow, white, and blue ellipsoids represent Mn, Fe, F, O, S, C, and N atoms, respectively; ellipsoids are shown at the 30% probability level. H atoms and triflate counteranions have been omitted for clarity.

Figure 2. Structure of [(cyclam$_2$^{i}PrO)Mn$_2$(μ-N$_3$)]$^{2+}$ in **5**. Purple, red, and blue ellipsoids represent Mn, O, and N atoms, respectively; ellipsoids are shown at the 30% probability level. H atoms and triflate counteranions have been omitted for clarity.

Table 1. Crystallographic Data[a] for Complexes **4**−**6**

	4	**5**	**6**
formula	$C_{26}H_{51}F_9Mn_2N_8O_9S_3$	$C_{25}H_{51}F_6Mn_2N_{11}O_6S_2$	$C_{26}H_{51}F_9Fe_2N_8O_{10}S_3$
fw	1012.81	905.77	1014.63
T, K	100	100	100
λ, Å	0.710 73	0.710 73	1.541 78
space group	*Pnma*	*P2$_1$/n*	*Pnma*
Z	4	2	4
a, Å	17.7548(10)	9.3083(7)	17.8273(3)
b, Å	13.6577(8)	13.9539(10)	13.4119(2)
c, Å	16.9173(9)	14.9380(11)	17.0929(3)
β, deg		99.3660(10)	
V, Å^3	4102.3(4)	1914.3(2)	4086.88(12)
d_{calcd}, g cm^{-3}	1.640	1.571	1.649
R1 (wR2),[b] %	6.74 (17.05)	8.83 (21.55)	8.11 (20.87)

[a] Obtained with graphite-monochromated Mo Kα radiation (**4** and **5**) and Cu Kα radiation (**6**). [b] R1 = $\Sigma||F_o| - F_c||/\Sigma|F_o|$; wR2 = $\{\Sigma[w(F_o^2 - F_c^2)^2]/\Sigma[w(F_o^2)^2]\}^{1/2}$.

Table 2. Selected Interatomic Distances (Å) and Angles (deg) for the Complexes in **4**−**6**

	4	**5**	**6**
M---M	3.841(3)	3.461(8)	3.778(7)
M−O(1)	2.131(3)	1.894(7)	2.03(2)
M−N(1), M−N(2), M−N(3), M−N(4)	2.265(3), 2.291(3), 2.294(3), 2.316(3)	2.135(9), 2.179(10), 2.288(18), 2.298(30)	2.135(6), 2.162(8), 2.176(8), 2.373(9)
M−X (N$_3$ or OTf)	2.269(2)	2.246(17)	2.277(4)
M−O(1)−M	128.6(4)	128.1(5)	136.7(5)
Mn−N(5)−Mn	n/a	87.2(6)	n/a

Table 3. Magnetic Behavior of the Dimanganese and Diiron Complexes

complex	μ_{eff} (μ_B)	J (cm^{-1})
4	8.0	−3.6
5	8.2	+0.1
6	7.0	−2.8

For compound **6**, the room temperature $\chi_M T$ value of 6.1 emu K mol^{-1} is consistent with the calculated value of 6.0 emu K mol^{-1} for two isolated high-spin d^6 octahedral $S = 2$ iron(II) centers. In this case, $\chi_M T$ falls to 0.55 emu K mol^{-1} at 4 K, and a fit to the data using a Hamiltonian of the form $\hat{H} = -2J'\hat{S}_{Fe(1)}\cdot\hat{S}_{Fe(2)}$ yielded a value for the exchange coupling of $J = -2.8$ cm^{-1}.[19] Compound **6** was EPR silent at 77 K in the X-band region. It is also worth noting that for compounds **4** and **6** the steady decrease in $\chi_M T$ values with temperature confirms that there is no contamination of the samples with mononuclear (cyclam)M(CF$_3$SO$_3$)$_2$ species
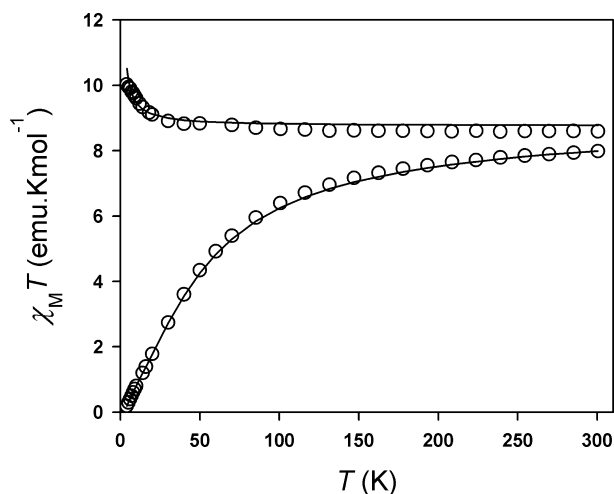
Figure 3. Magnetic data for compounds **4** (bottom) and **5** (top) in an applied field of 1 kG. Circles represent the experimental data, and solid lines represent best fits to the data using *MAGFIT3.0*.

(where M = Mn or Fe). This has been reported as a problem in the synthesis of similar isopropoxide-bridged tacn (tacn = 1,4,7-triazacyclononane) complexes.[20]

Electrochemical Measurements. Cyclic voltammetry experiments for complex **4** (Figure 5) revealed one-electron, reversible oxidation events at $E_o' = +0.79$ V ($\Delta E_p = 130$ mV) and $E_o' = +1.06$ V ($\Delta E_p = 123$ mV) and two unresolved, one-electron oxidation events at $E_o' = +1.51$ V ($\Delta E_p = 160$ mV) vs SCE in acetonitrile (0.1 M Bu$_4$NClO$_4$). These were assigned to the Mn$^{II}_2$/Mn^{II}Mn^{III}, Mn^{II}Mn^{III}/Mn$^{III}_2$, and Mn$^{III}_2$/Mn$^{IV}_2$ couples, respectively (Table 4). The large peak separation for the final redox couple, of $\Delta E_p = 160$ mV, implicates two overlapping one-electron processes rather than a two-electron event. Overall, the data indicate that four electrons can be reversibly removed from the complex over a spread of 0.72 V, the final three electrons within 0.45 V. The observed 0.72 V spread of the four-electron redox processes observed in **4** is relatively narrow by comparison to other dimanganese complexes reported to date: in [(Mn-(bpia)(Cl))$_2$(μ-O)](ClO$_4$)$_2$·2MeCN [where bpia = bis(pico-lyl)(*N*-methylimidazol-2-yl)amine],[9] these redox couples are spread over 0.91 V. Under identical conditions, electrochemical measurements on mononuclear [cyclamMn(MeCN)$_2$]-(CF$_3$SO$_3$)$_2$ (**7**) reveal one one-electron, reversible oxidation wave at +0.86 V, which we assign to the Mn^{II}/Mn^{III} couple (Figure S1 in the Supporting Information). The data suggest

(18) (a) Abragam, A.; Bleaney, B. *Electron Paramagnetic Resonance of Transition Ions*; Clarendon: Oxford, U.K., 1970; pp 138. and 158. (b) Mathur, P.; Crowder, M.; Dismuskes, G. C. *J. Am. Chem. Soc.* **1987**, *109*, 5227.
(19) Unlike for the isotropic high-spin d^5 manganese(II) compounds, the fit to the data for compound **6** is not ideal. This most likely results from an orbital contribution to the moment that is commonly observed for the iron(II) electronic configuration;[17] no effort was made to account for this in order to obtain a better fit. Carlin, R. L. *Magnetochemistry*; Springer-Verlag: Berlin, Germany, 1986; p 65.
(20) Warren, M.; Battle, A. R.; Moubaraki, B.; Murray, K. S.; Spiccia, L.; Skelton, B. W.; White, A. H. *Dalton Trans.* **2004**, 2309.
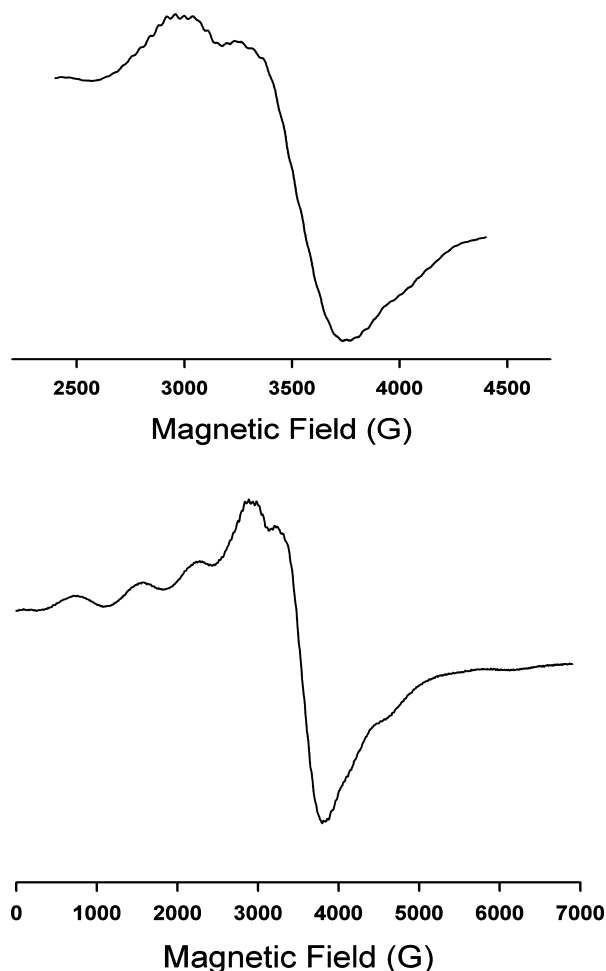
Figure 4. X-band EPR spectrum of **4** (bottom) and an expanded spectrum showing ⁵⁵Mn hyperfine coupling (top). Both spectra were recorded using 1 mM solutions of **4** in MeOH/toluene (1:1) at 77 K: microwave power, 1.0 mW; microwave frequency, 9.68 GHz; modulation amplitude, 10 G; gain, 31 000.
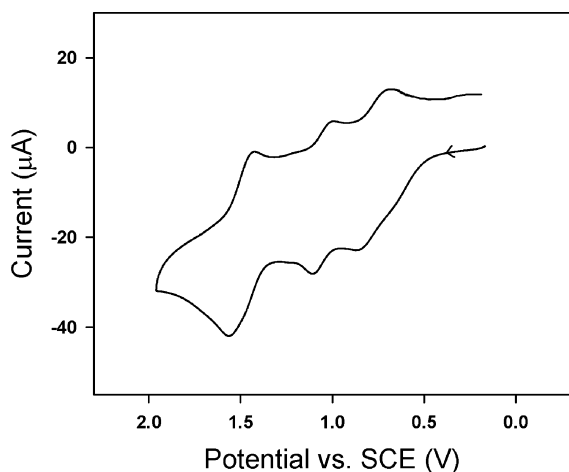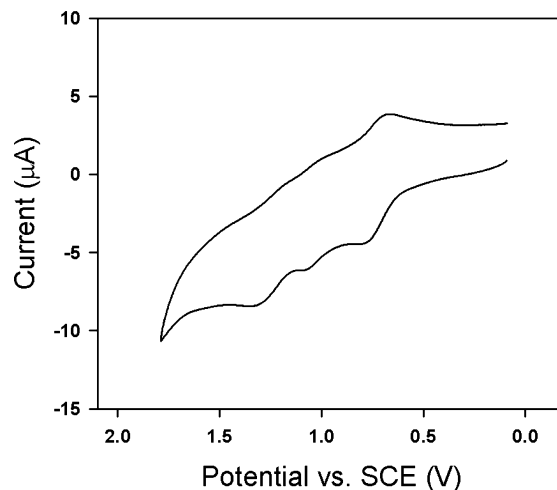

Figure 5. Cyclic voltammogram for a 1 mM solution of complex **4** in MeCN.

that electronic coupling of the metal centers via the isopropoxide bridge lowers the potential of the first $Mn^{II} \rightarrow Mn^{III}$ oxidation and raises the potential of the second $Mn^{II} \rightarrow Mn^{III}$ oxidation compared with that of mononuclear [cyclamMn-$(CF_3SO_3)_2]^{2+}$. However, it should be noted that the coordination sphere around Mn in the dinuclear system is slightly

Table 4. Redox Potentials (vs SCE) for 1 mM Solutions of the Dimanganese and Diiron Complexes in MeCN (0.1 M Bu₄NClO₄)

complex	redox couple	potential (V)	peak separation (mV)
4	$Mn^{II}_2/Mn^{II}Mn^{III}$	0.79	130
	$Mn^{II}Mn^{III}/Mn^{III}_2$	1.1	123
	Mn^{III}_2/Mn^{IV}_2	1.5	160
5	$Mn^{II}_2/Mn^{II}Mn^{III}$	0.74	135
	$Mn^{II}Mn^{III}/Mn^{III}_2$	1.1	a
	Mn^{III}_2/Mn^{IV}_2	1.4	a
6	$Fe^{II}_2/Fe^{II}Fe^{III}$	0.43	80
	$Fe^{II}Fe^{III}/Fe^{III}_2$	0.88	114
	$Fe^{III}_2/Fe^{III}Fe^{IV}$	1.8	a
	$Fe^{III}Fe^{IV}/Fe^{IV}_2$	1.9	a

^{a} This process was irreversible, and the potential quoted refers to the oxidation potential.
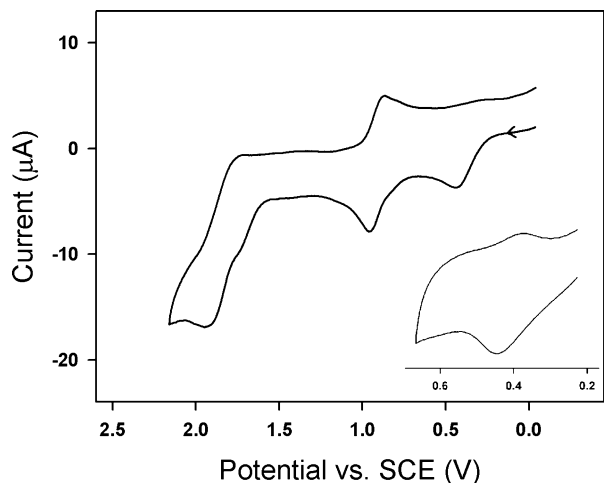

Figure 6. Cyclic voltammogram for a 1 mM MeOH solution of complex **5**.

different because it contains half a negatively charged isopropoxide ligand per metal center, which is expected to shift the potentials slightly negatively. While only one reversible wave was observed for [cyclamMn(MeCN)₂]²⁺, a more rigid manganese complex of a cyclam derivative [CBcyclamMnCl₂] (where CBcyclam = 4,11-dimethyl-1,4,8,11-tetraazabicyclo[6.6.2]hexadecane is a very rigid cyclam derivative), reported by Busch and co-workers, displays two one-electron redox couples in aqueous solution corresponding to the Mn^{II}/Mn^{III} and Mn^{III}/Mn^{IV} events.[21] Both [CBcyclamMnCl₂] and **4** possess facially coordinated cyclam moieties, while the cyclam ligand in [cyclamMn-(MeCN)₂]²⁺ has the trans configuration.

Upon replacement of the triflate counteranion with the single-atom bridge of azide in **5**, only one of the redox events observed in **4** remains reversible (Figure 6). In **5**, four electrons are removed within 0.65 V, a slightly narrower window than that observed for **4**, and each of the events is at slightly lower potential (by 0.05−0.2 V) compared with those observed for **4**. The first couple is reversible and occurs at 0.74 V ($\Delta E_p = 135$ mV), a one-electron, irreversible oxidation event occurs at 1.11 V, and a two-electron, irreversible oxidation event is observed at 1.38 V vs SCE.

(21) Hubin, T. J.; McCormick, J. M.; Collinson, S. R.; Buchalova, M.; Perkins, C. M.; Alcock, N. W.; Kahol, P. K.; Raghunathan, A.; Busch, D. H. *J. Am. Chem. Soc.* **2000**, *122*, 2512.
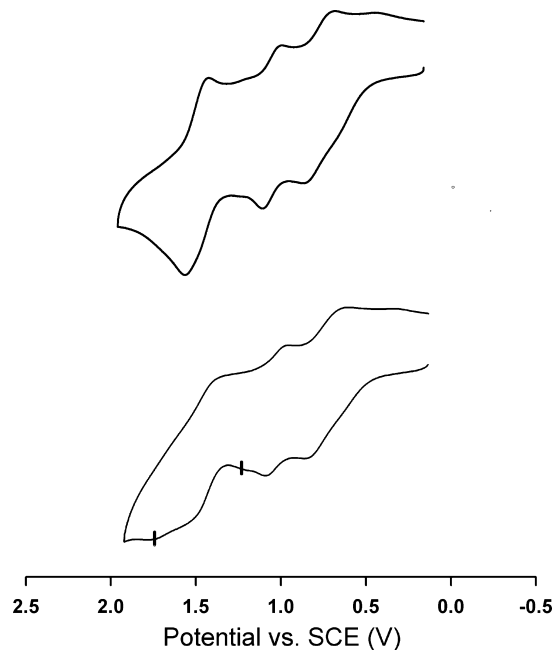
Figure 7. Cyclic voltammogram for a 1 mM solution of complex **6** in MeCN scanned at 100 mV s^{-1}. The inset shows the first redox couple scanned at 1000 mV s^{-1}.

Cyclic voltammetry experiments for complex **6** (Figure 7) reveal two one-electron, reversible and two one-electron, irreversible oxidation events. The first oxidation wave is irreversible when the voltage is scanned to high potentials before the reductive scan. However, when the voltage is reversed before the second oxidation event, the couple becomes partially reversible (Figure 7, inset) and is assigned as the Fe$^{II}_2$/Fe^{II}Fe^{III} couple: $E_o' = +0.43$ V ($\Delta E_p = 80$ mV). The remaining redox events occur at $+0.88$ V ($\Delta E_p = 80$ mV), $E_o' = +1.77$ V, and $E_o' = +1.97$ V vs SCE, and only the first of these is reversible. These were assigned to the Fe^{II}Fe^{III}/Fe$^{III}_2$, Fe$^{III}_2$/Fe^{III}Fe^{IV}, and Fe^{III}Fe^{IV}/Fe$^{IV}_2$ couples, respectively. The data indicate that the first two redox events occur at lower potentials than those for the corresponding dimanganese complex **4**, as would be expected for a diiron analogue. However, the final two irreversible events occur at higher potentials than the corresponding oxidations in **4**.

Behavior of Complexes 4 and 6 in Aqueous Solution. In aqueous solutions, complexes **4** and **6** exhibit very low solubility. However, in aqueous solutions containing roughly 50% MeCN or 10% DMF, they are appreciably soluble. EPR spectra were collected on 1 mM MeCN solutions of **4** containing 20% water at 77 K in order to confirm the stability of the complex in the aqueous environment. As illustrated in Figures S4 and S5 in the Supporting Information, the spectrum of **4** in MeCN/water (8:2) is as expected for two exchange-coupled Mn^{II} ions; the compound has not dissociated into isolated manganese(II) centers, as has been observed for other isopropoxide-bridged manganese(II) dimers that have been reported.[22] Presumably, the more rigid chelating cyclam ligands employed here provide more stability than that in the aforementioned examples. The spectrum exhibits some differences with respect to the spectrum collected in neat MeCN. This may be a result of some change in the coordination sphere of the Mn^{II} ions such as a water ligand binding to the metal center in place of the triflate counteranion. Complex **6** could not be investigated in the same

(22) Boelrijk, A. E. M.; Khangulov, S. V.; Dismukes, G. C. *Inorg. Chem.* **2000**, *39*, 3009.

Figure 8. Cyclic voltammogram for a 1 mM solution of complex **4** in MeCN (top) and cyclic voltammogram recorded in the presence of 15 mM water (bottom). Positively shifted shoulders on the oxidative peaks (marked by a vertical line) imply that neutral H$_2$O is binding in place of the negatively charged triflate counteranion.[23]

manner because of its EPR-silent nature, as expected for integer-spin iron(II) centers.
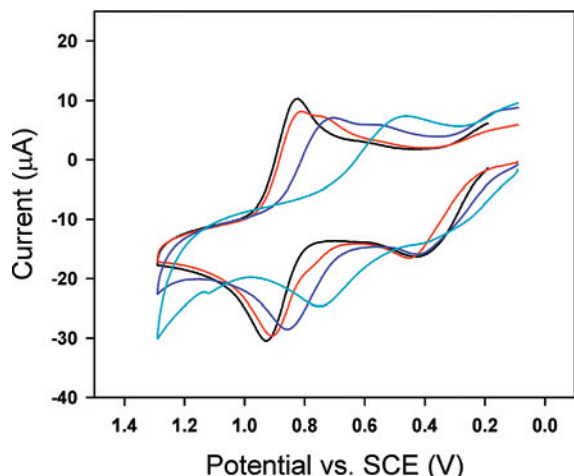
In order to further investigate the interactions of **4** and **6** with water, cyclic voltammetry experiments were carried out. Inclusion of water in the electrochemical study of **4** (vide supra) results in a shift in the peak potentials to more positive values; the voltammogram of **4** in the presence of 15 equiv of water is shown in Figure 8. The observation of a second set of peaks in addition to that of the parent compound is consistent with a neutral water ligand binding the manganese centers in place of the anionic triflate ligand.[23] For the Mn^{II}Mn^{III}/Mn$^{III}_2$ and Mn$^{III}_2$/Mn$^{IV}_2$ couples, the oxidation potentials of the putative **4**·H$_2$O adduct can be distinguished from those of **4**. The Mn^{II}Mn^{III}/Mn$^{III}_2$ oxidation wave for **4**·H$_2$O is seen as a shoulder on the peak for **4** at $+1.29$ V (compared with $+1.12$ V for **4**), and the Mn$^{III}_2$/Mn$^{IV}_2$ oxidation wave for **4**·H$_2$O is seen at $+1.83$ V (compared with $+1.59$ V for **4**). These results indicate that although complex **4** is insoluble in water, interaction of water as a substrate to the dimanganese complex in nonaqueous solvents probably occurs.[24] No evidence for electrocatalytic O$_2$ evolution was observed.

Inclusion of water in the electrochemical experiment of **6** also resulted in the appearance of additional peaks (vide supra), in this case for both the oxidative and reductive processes. Figure 9 shows the cyclic voltammogram for the

(23) It is possible that the initial species in solution contains acetonitrile bound to the metal center rather than triflate. In either case, the shift in the peak potential after water is added indicates that some interaction with the water has taken place.
(24) The observation of a distinct peak in addition to the parent peak, rather than a shift of the parent peak, implies that the observation is not simply the result of a change in the dielectric constant of the solvent causing a shift of the relevant redox couples.

measured were limited by the maximum concentration of H_2O_2 that could be achieved in a given solution. The rate for this reaction was estimated volumetrically at 12.6 mol of H_2O_2 s^{-1} mol cat.$^{-1}$ for a period of 10 min. The direct comparison of these rates with literature values is difficult because the latter are generally reported for the first moments of a reaction via electrode-detected methods. Of interest in the current system is the consistent catalase activity achieved for over 1 h until the activity drops as a result of the depletion of H_2O_2 in the reaction solution (Figure S4 in the Supporting Information). This prolonged activity illustrates the stability of the multidentate and saturated amine donor ligand system under highly oxidizing conditions.

Attempts to chemically oxidize complex **4** to a Mn^{III}_2 or Mn^{IV}_2 species using strong oxidants such as $NOPF_6$ resulted in the formation of orange solutions, from which no well-defined products could be identified. The reaction of **4** with 190 equiv of PhIO in acetonitrile also resulted in the formation of an orange solution and the consumption of all of the PhIO (Table 5). This was measured by the amount of PhI formed (via ^1H NMR spectroscopy). Although the metal-containing decomposition products of these reactions could not be identified, IR spectroscopy reveals that the absorption bands corresponding to the triflate anion are not split anymore. This indicates that the triflate anion is no longer bound to the Mn ions. The UV−visible spectrum consisted of high-energy charge-transfer bands. EPR spectroscopy revealed a six-line spectrum ($A = 101 \pm 7$ G) consistent with the presence of uncoupled, isotropic Mn^{II} ions (Figure S5 in the Supporting Information). The observation of an EPR signal does not rule out the possibility that manganese(III) monomers or dimers are also present because such species would be EPR-silent. The presence of isolated Mn^{II} ions could be attributed to degradation of the ligand isopropoxide bridge or simply to dissociation of the isopropoxide ligand from at least one of the manganese centers. When the same reaction was performed in the presence of 250 equiv of styrene (Table 5), 190 equiv of PhIO was consumed along with the formation of styrene epoxide in 80% yield (with respect to PhIO consumed). The reactivity observed for **4** under oxidizing conditions is in contrast to that documented for mononuclear (cyclam)MnL_2 complexes (where L = anionic ligand):[26] syntheses directed at (cyclam)MnL_2 complexes under aerobic conditions generally result in the formation of the mixed-valent manganese(III/IV) thermodynamic sink [(cyclam)Mn]$_2(\mu$-O)$_2$.

The diiron(II) compound **6** exhibits different reactivity compared to **4** in the presence of PhIO and H_2O_2 (Table 5). Reaction with either stoichiometric PhIO or H_2O_2 results in

Figure 9. Cyclic voltammogram for a 1 mM solution of complex **6** in MeCN (black) and the same solution containing 30 mM water (red), 1 M water (blue), and 5 M water (green). Negatively shifted shoulders on the reductive peaks imply that neutral H_2O is binding in place of the negatively charged triflate counteranion or an acetonitrile solvate molecule.

Table 5. TONs for Consumption of PhIO, Epoxidation of Styrene, and Catalase Activity in the Presence of **4** and **6**[a]

catalyst/ cocatalyst	oxidant	TON, oxidant consumed	TON, styrene oxide produced	% oxidant consumed transferred to substrate
4	PhIO	190	b	
4	PhIO	190	150	80
4	H_2O_2	20 000	b	
4	H_2O_2	nd	0	0
6	PhIO	110	b	
6	PhIO	80	32	40
6	H_2O_2	0	b	

[a] Reaction conditions: 1.25 mg of **4** or **6**, 1 mL of CD$_3$CN, 4 μL of toluene internal standard, 190 equiv (50 mg) of PhIO or 20 000 equiv of H_2O_2, 250 equiv of styrene (32 mg, where added), 16 h of reaction time. [b] No styrene was added to this reaction. nd = not determined. Numbers reported are an average taken from reactions run in duplicate.

experiment performed in the presence of 30 equiv of water. Upon the addition of 30 equiv of water, a shoulder appeared on the reductive wave of the $Fe^{II}Fe^{III}/Fe^{III}_2$ couple, suggesting that H_2O binds the diiron core in the Fe^{III}_2 oxidation state. The addition of further equivalents of water resulted in an additional and further cathodically shifted set of peaks for both the oxidative and reductive processes, suggesting that a second 1 equiv of water binds the diiron core. When the concentration of water in the solution reached 10%, only one wave was observed at a potential that was 0.37 V negative of the original couple: +0.61 V ($\Delta E_p = 320$ mV). In both the dimanganese complex (**4**) and the diiron complex (**6**), observation of two peaks rather than one averaged peak at low concentrations of water (15−30 mM) suggests that exchange of the triflate and H_2O ligands is slow on the electrochemical time scale.

Reactivity of Complexes 4 and 6 with Oxidants. Compound **4** reacts with H_2O_2 with vigorous evolution of O_2 (Table 5). Catalase efficacy in dimanganese complexes is well-docmented, and the turnover number (TON) of ∼20 000 reported here represent a highly active system.[11,25] The activity of the complex appeared only to diminish when H_2O_2 had been depleted from the reaction solution, and TONs

(25) (a) Mathur, P.; Crowder, M.; Dismukes, G. C. *J. Am. Chem. Soc.* **1987**, *109*, 5227. (b) Bossek, U.; Wieghardt, K.; Nuber, B.; Weiss, J. *Inorg. Chim. Acta* **1989**, *165*, 123. (c) Bossek, U.; Saher, M.; Weyhermueller, M.; Wieghardt, K. *Chem. Commun.* **1992**, 1780. (d) Boelrijk, A. E. M.; Dismukes, G. C. *Inorg. Chem.* **2000**, *39*, 3020. (e) Godbole, M. D.; Kloskowski, M.; Hage, R.; Rompel, A.; Mills, A. M.; Spek, A. L.; Bouwman, E. *Eur. J. Inorg. Chem.* **2005**, 305.
(26) (a) Brewer, K. J.; Calvin, M.; Lumpkin, R. S.; Otvos, J. W.; Spreer, L. O. *Inorg. Chem.* **1989**, 4446. (b) Daugherty, P. A.; Glerup, J.; Goodson, P. A.; Hodgson, D. J.; Michelsen, K. *Acta Chem. Scand.* **1991**, *45*, 244. (c) Mossin, S.; Sorensen, H. O.; Weihe, H.; Glerup, J.; Sotofte, I. *Inorg. Chim. Acta* **2005**, *358*, 1096.

the formation of deep-red solutions at −35 °C in MeCN; no evidence for gaseous O_2 evolution was observed in the reactions of **6** with H_2O_2. The reaction of **6** with 190 equiv of PhIO at room temperature yielded 110 equiv of PhI, and a dark-red powder was isolated after PhI was removed by washing with pentane. As in the case of **4**, IR spectroscopy revealed that the triflate counteranion was no longer coordinated to the iron center. In addition to high-energy charge-transfer bands, the UV−visible spectrum revealed two overlapping bands at 530 nm (ϵ = 360 L mol cm^{-1}) and 565 nm (ϵ = 340 L mol cm^{-1}), which are characteristic in energy and extinction coefficient with oxo-bridged diiron(III) complexes (Figure S6 in the Supporting Information).[27] When the reaction of **6** with 190 equiv of PhIO was performed in the presence of styrene, only 40% of the total PhIO consumed was transferred to yield styrene oxide; this is in contrast to **4**, for which the yield with respect to PhIO was 80%. Efforts to further characterize the red product from oxidation reactions with the diiron complex are ongoing.

Conclusions. Dimanganese and diiron complexes of a binucleating cyclam ligand have been synthesized in which the metal centers are structurally and electronically coupled via an isopropoxide linker incorporated into the ligand framework. Structural studies indicate that this scaffold provides a flexible binding pocket between the two metal centers. When the one-atom-bridging ligand azide is employed, a 0.38 Å shortening of the Mn---Mn distance is observed compared with that of the parent triflate compound. Cyclic voltammetry measurements demonstrate that the hard donor amine ligands impart high oxidation potentials to the metal centers and that the incorporation of two electronically coupled metal centers within the complexes results in accessible four-electron redox activity. For the dimanganese complex, the redox events are all reversible and occur within 0.72 V at high enough potentials to be of interest for water oxidation chemistry. The diiron complex displays four one-electron couples, of which two are reversible. In accordance with the observed reversibility and relative redox potentials of the complexes, the dimanganese complex is more efficient at mediating O-atom transfer to styrene. On the basis of the accessible four-electron redox chemistry of the compounds and their ability to facilitate O-atom transfer reactions to styrene, ongoing studies will investigate the possibility of radical coupling of M^{IV}O moieties with a view toward O−O bond formation.

Experimental Section

Preparation of Compounds. All manipulations were carried out using standard Schlenk or glovebox techniques under a N_2 atmosphere. Unless otherwise noted, solvents were deoxygenated and dried by thorough sparging with N_2 gas followed by passage through an activated alumina column. Deuterated solvents were purchased from Cambridge Isotopes Laboratories, Inc., and were degassed and stored over activated 3 Å molecular sieves prior to use. The compounds Mn(CF$_3$SO$_3$)$_2$,[26c] Fe(CF$_3$SO$_3$)$_2$·2MeCN,[28]

cyclam-Boc$_3$,[29] and PhIO[30] were prepared according to literature procedures. All other reagents were purchased from commercial vendors and used without further purification.

X-ray Structure Determinations. X-ray diffraction studies were carried out on a Bruker Circle 3 diffractometer equipped with a CCD detector. Measurements were carried out at −175 °C using Mo Kα (λ = 0.710 73 Å) radiation for **4** and **5** and Cu Kα (λ = 1.541 78 Å) radiation for **6**. Crystals were mounted on a Kaptan loop with Paratone-N oil. The initial lattice parameters were obtained from a least-squares analysis of more than 100 centered reflections; these parameters were later refined against all data. Data were integrated and corrected for Lorentz polarization effects using *SAINT* and were corrected for absorption effects using *SADABS2.3*.

Space group assignments were based upon systematic absences, *E* statistics, and successful refinement of the structures. Structures were solved by direct methods with the aid of successive difference Fourier maps and were refined against all data using the *SHELXTL 5.0* software package. Thermal parameters for all non-H atoms were refined anisotropically except for some of the disordered C atoms in the macrocycle rings of **4**−**6**. H atoms, where added, were assigned to ideal positions and refined using a riding model with an isotropic thermal parameter 1.2 times that of the attached C atom (1.5 times for methyl hydrogens). In **4** and **6**, all atoms in the cyclam rings are disordered over two positions, with the two- and three-carbon bridges alternating position in the different orientations. The two conformations were refined to occupancies of 0.8:0.2 and 0.6:0.4 in **4** and **6**, respectively. H atoms were added to the major conformation only. The isopropoxide bridge is also disordered over two positions. In **5**, the dimer is disordered over two orientations, of equal occupancy, by rotation of 180° across the Mn---Mn axis. There are two positions for every atom except the manganese centers. C−O bonds in the isopropoxide were restrained to be similar to those in **4** so that the N atoms of the azide unit could be refined to fill the remaining electron density. Depictions of the disordered structures are shown in the Supporting Information (Figures S7−S9). For clarity, ball-and-stick drawings are shown, H atoms have been removed, and only the atoms of the major conformation are labeled.

Other Physical Measurements. Elemental analyses were performed by Robinson Microlit Laboratories. ^{1}H and ^{13}C NMR spectra were recorded at ambient temperature using a Varian 300 MHz spectrometer; chemical shifts were referenced to the residual solvent. IR measurements were obtained on samples prepared as KBr pellets using a Bio-Rad Excalibur FTS 3000 spectrometer. Mass spectra were collected using a Bruker Daltonics APEXIV 4.7 T Fourier transform ion cyclotron resonance mass spectrometer equipped with an electrospray ionization source. Electrochemical measurements were recorded in a glovebox under a N_2 atmosphere using a CH Instruments electrochemical analyzer, a glassy carbon or a platinum working electrode, a platinum wire auxiliary electrode, and an Ag/AgNO$_3$ nonaqueous reference electrode. Reported potentials are all referenced to the SCE couple and were determined using ferrocene as an internal standard. The number of electrons passed in a given redox process was estimated by comparison of the peak current with the peak current of ferrocene included as an internal standard. X-band EPR measurements were recorded using a Bruker EMX spectrometer. Solution spectra were acquired in MeOH/toluene (1:1) or acetonitrile. Samples were prepared in a glovebox under N_2 in quartz EPR tubes equipped with J. Young caps. Magnetic measurements were recorded using a Quantum Designs

(27) Tshuva, E. Y.; Lippard, S. J. *Chem. Rev.* **2004**, *104*, 987.
(28) Hagen, K. S. *Inorg. Chem.* **2000**, *39*, 5867.

(29) Brandes, S.; Gros, C.; Denat, F.; Pullumbi, P.; Guilard, R. *Bull. Soc. Chem. Fr.* **1996**, *133*, 65.
(30) Saltzmann, H.; Sharefkin, J. G. *Org. Synth.* **1973**, *5*, 658.

MPMS XL magnetometer at 1000 G. The sample was contained under nitrogen in polycarbonate caps sealed with Teflon tape and suspended in the magnetometer in a plastic straw. The magnetic susceptibility was adjusted for diamagnetic contributions using the constitutive corrections of Pascal's constants.

1,3-Bis(Boc₃-cyclam)-2-hydroxypropane (1). 1,3-Dibromopropanol (4.15 mL, 41.6 mmol) and triethylamine (12.3 mL, 105 mmol) were added via syringe to Boc₃-cyclam (34.8 g, 83.0 mmol), which was dissolved in dry acetonitrile (800 mL). The solution was heated at reflux, and the progress of the reaction was monitored by ^{13}C NMR. After 3 days, a further 0.5 mL of 1,3-dibromopropanol was added to the reaction mixture, and after 6 days, when all of the starting material had been consumed, the reaction was cooled to room temperature. The solvent was removed by rotary evaporation to afford an oily residue. The oil was dissolved in 800 mL of chloroform and washed with 10% aqueous NaOH (3 × 800 mL) and water (2 × 800 mL), and then the solution was dried over Na_2SO_4 and the solvent removed under vacuum. The resulting oil was dissolved in a minimum amount of hexanes and purified on a silica gel column using 30:70 (v/v) hexanes/ethyl acetate as the eluent under flash chromatography conditions. The fractions containing **1** were combined, and the solvent was removed under vacuum to yield 17.4 g (45%) of product as a viscous oil. ^{1}H NMR spectroscopy displayed many broad, overlapping signals that provided no useful information. ^{13}C{^{1}H} NMR (300 MHz, $CDCl_3$): δ 156, 155 (s, *C*=O Boc), 79.5 (s, *C*H(OH) propane), 65.0 (s, *C*H₂ propane), 60.2, 59.9, 53.7, 52.1, 47.5, 46.7, 46.0, 45.7 (s, *C*H₂ ring carbons), 28.3 (s, *C*H₃ Boc). ESI$^+$-MS (CH₃Cl): m/z 1057 ([**1** + H]$^+$).

1,3-Bis(cyclam)-2-hydroxypropane·9HCl (2). A 1:1 (v/v) solution of 12 M HCl and ethanol (60 mL) was poured onto **1** (17.4 g, 16.4 mmol). The resulting solution quickly yielded a white precipitate, and the suspension was then stirred for 1 h. The solid was collected by filtration and washed with ethanol (30 mL). The sticky white solid was washed by stirring in a 1:2 (v/v) solution of 12 M HCl and ethanol (60 mL) for 1 h. The resulting white solid was collected by filtration, washed with ethanol (60 mL), and dried under vacuum overnight to afford 11.1 g (87%) of **2**. ^{1}H NMR (300 MHz, D_2O): 3.36 (tt, 1H, CH propane), 3.42 (m, 16H, α-CH₂), 3.20 (m, 16H, α-CH₂), 3.05 (dd, 4H, CH₂ propane), 1.99 (m, 8H, β-CH₂). ^{13}C{^{1}H} NMR (300 MHz, D_2O): 61.5 (s, *C*H(OH) propane), 57.4 (s, *C*H₂ propane), 49.0, 45.8, 41.7, 41.3, 41.1, 37.8, 37.5 (s, α-CH₂), 18.8. 18.6 (s, β-CH₂). ESI$^+$-MS: m/z 457 [**2** − 9HCl + H]$^+$.

1,3-Bis(cyclam)-2-hydroxypropane (3). An aqueous 16 M NaOH solution was added dropwise to **2** (11.1 g, 14.2 mmol), which was dissolved in 10 mL of water until the solution reached pH = 13. The aqueous solution was extracted with chloroform (6 × 50 mL), and the combined extracts were dried over Na_2SO_4. The solvent was removed under vacuum to afford 5.20 g of **3** as a white solid (81% yield). ^{1}H NMR (300 MHz, $CDCl_3$): 3.65 (quint, 1H, CH propane), 2.65 (m, 32H, α-CH₂), 2.40 (d, 4H, CH₂ propane), 1.82 (m, 2H, β-CH₂), 1.66 (m, 6H, β-CH₂). ^{13}C{^{1}H} NMR (300 MHz, $CDCl_3$): 77.2 (s, *C*H(OH) propane), 68.2 (s, *C*H₂ propane), 59.0, 56.4, 55.3, 50.9, 49.3, 48.5, 47.8, 47.7 (s, α-CH₂), 28.5, 26.3 (s, β-CH₂). ESI$^+$-MS: m/z 457 [**3** + H]$^+$. Anal. Calcd for $C_{23}H_{52}N_8O$: C, 60.48; H, 11.48; N, 24.53. Found: C, 59.90; H, 11.67; N, 24.33.

[(cyclam₂^{i}PrO)Mn₂(μ-CF₃SO₃)](CF₃SO₃)₂ (4). A solution of Mn(CF₃SO₃)₂ (622 mg, 1.80 mmol) in MeCN (10 mL) was added to a suspension of **3** (400 mg, 0.880 mmol) in MeCN (10 mL), and the resulting pale-yellow solution was stirred for 16 h. Triethylamine (0.12 mL) was added, and the solution was stirred

for 1 h before being filtered through Celite. The solvent was removed under vacuum, the resulting oily residue was dissolved in MeCN (10 mL) and the solution filtered through Celite. Colorless crystals of **4** (705 mg, 70%) suitable for X-ray diffraction anaylsis were obtained by diffusion of diethyl ether into the MeCN solution. Anal. Calcd for $C_{26}H_{51}F_9Mn_2N_8O_{10}S_3$: C, 31.02; H, 4.51; N, 11.13. Found: C, 30.84; H, 4.80; N, 10.93. IR (KBr): ν_{NH} 3265 m, ν_{SO} 1286 s, 1249 s, 1226 s cm^{-1}. ESI$^+$-MS: m/z 863 [**4** − CF₃SO₃]$^+$. μ_{eff} = 8.0 μ_B.

[(cyclam₂^{i}PrO)Mn₂(μ-N₃)](CF₃SO₃)₂ (5). A solution of **4** (40.0 mg, 0.040 mmol) in 2 mL of MeCN was stirred with NaN₃ (26.0 mg, 0.20 mmol) for 16 h. The excess, insoluble NaN₃ was then removed by filtering the mixture through Celite. Colorless crystals of **5** suitable for X-ray analysis were obtained by diffusion of diethyl ether into the MeCN solution (21.1 mg, 58%). Anal. Calcd for $C_{25}H_{51}F_6Mn_2N_{11}O_7S_2$: C, 33.37; H, 5.04; N, 17.13. Found: C, 33.37; H, 5.44; N, 16.53. IR (KBr): ν_{NH} 3265 m, ν_{NN} 2058 s, ν_{SO} 1286 s, 1245 s, 1226 m cm^{-1}. μ_{eff} = 8.3 μ_B.

[(cyclam₂^{i}PrO)Fe₂(μ-CF₃SO₃)](CF₃SO₃)₂ (6). A solution of **3** (100 mg, 0.220 mmol) in MeOH (2 mL) was added to a solution of Fe(CF₃SO₃)₂·2MeCN (192 mg, 0.440 mmol) in MeOH (2 mL). The resulting pale-yellow mixture was stirred for 16 h before it was filtered through Celite. Colorless crystals of **7** (180 mg, 81%) suitable for X-ray diffraction analysis were obtained by diffusion of diethyl ether into the MeOH solution. Anal. Calcd for $C_{26}H_{51}F_9Fe_2N_8O_{10}S_3$: C, 30.96; H, 4.50; N, 11.11. Found: C, 31.28; H, 4.91; N, 11.02. IR(KBr): ν_{NH} 3260, ν_{SO} 1285 s, 1251 s, 1227 m cm^{-1}. μ_{eff} = 6.1 μ_B.

[(cyclam)Mn(CF₃SO₃)₂] (7). Cyclam (300 mg, 1.5 mmol) and Mn(CF₃SO₃)₂ (529 mg, 1.5 mmol) in 15 mL of MeCN were stirred and heated at 40 °C for 1 h. The solution was filtered and the solvent removed under vacuum. The residue was redissolved in MeCN and crystallized by diffusion of ether vapor into the solution (460 mg, 50%). Anal. Calcd for $C_{16}H_{26}F_6MnN_6O_6S_2$: C, 26.24; H, 3.67; N, 10.20. Found C, 26.23; H, 4.28; N, 10.06. IR(KBr): ν_{NH} 3266, ν_{SO} 1242 s, 1219 s cm^{-1}.

Oxidation Reactions of 4 and 6. Product yields and TONs were determined by NMR spectroscopy using toluene as an internal standard.

Reaction of 4 with PhIO. Solid PhIO (50 mg, 0.23 mmol) was added to a solution of **4** (1.2 mg, 0.0012 mmol) dissolved in 1 mL of CD₃CN containing 4 μL of toluene as an internal standard. The reaction was stirred for 16 h and then filtered through Celite to remove unreacted PhIO.

Reaction of 6 with PhIO. Solid PhIO (100 mg, 0.23 mmol) was added to a solution of **7** (5.0 mg, 0.0049 mmol) dissolved in 1 mL of CD₃CN containing 4 μL of toluene as an internal standard. The reaction was stirred for 16 h and then filtered through Celite to remove unreacted PhIO. In order to isolate the iron-containing product of this reaction, the solvent was removed under vacuum and the oily residue washed twice with 5 mL of pentane. The dark-red solid was dried briefly under vacuum to give approximately 4 mg of the compound. Absorption spectrum (MeCN) [λ, nm (ϵ, L mol^{-1}cm^{-1})]: 565 (340), 530 (360).

Reaction of 4 and 6 with PhIO and Styrene. Solid PhIO (50 mg, 0.23 mmol) was added to a solution of complex **4** or **6** (1.2 mg, 0.0012 mmol) and styrene (32 mg, 0.31 mmol) dissolved in 1 mL of CD₃CN containing 4 μL of toluene as an internal standard. The reaction was stirred for 16 h and then filtered through Celite to remove unreacted PhIO.

Reaction of 4 with H₂O₂ and Quantification of O₂ Evolution. Disproportionation reactions were performed at room temperature in a sealed (PTFE septum) 10 mL round-bottomed flask

immersed in a water bath and equipped with a magnetic stir bar and a capillary gas delivery tube linked to an inverted graduated cylinder filled with water. The flask was charged with **4** (0.1 mL, 1 mmol; 10 mM MeCN solution) and 1.3 mL of MeCN. H_2O_2 (3.7 mL, 29.8 mmol; 10.4 M (30%) aqueous solution) was added via a syringe, and the reaction mixture was stirred vigorously. The time was set to zero immediately after the addition of H_2O_2. The conversion was monitored volumetrically, and the amount of O_2 produced was calculated using the ideal gas law.